Molecular Neurobiology (2019) 56:1461–1474
https://doi.org/10.1007/s12035-018-1158-x

GABA-B1 Receptor-Null Schwann Cells Exhibit Compromised In Vitro Myelination

Alessandro Faroni[1] · Simona Melfi[2] · Luca Franco Castelnovo[2] · Veronica Bonalume[2] · Deborah Colleoni[2] · Paolo Magni[2] · Marcos J. Araúzo-Bravo[3,4] · Rolland Reinbold[5] · Valerio Magnaghi[2]

Received: 15 February 2018 / Accepted: 28 May 2018 / Published online: 12 June 2018

Abstract

GABA-B receptors are important for Schwann cell (SC) commitment to a non-myelinating phenotype during development. However, the P0-GABA-B1$^{fl/fl}$ conditional knockout mice, lacking the GABA-B1 receptor specifically in SCs, also presented axon modifications, suggesting SC non-autonomous effects through the neuronal compartment. In this in vitro study, we evaluated whether the specific deletion of the GABA-B1 receptor in SCs may induce autonomous or non-autonomous cross-changes in sensory dorsal root ganglia (DRG) neurons. To this end, we performed an in vitro biomolecular and transcriptomic analysis of SC and DRG neuron primary cultures from P0-GABA-B1$^{fl/fl}$ mice. We found that cells from conditional P0-GABA-B1$^{fl/fl}$ mice exhibited proliferative, migratory and myelinating alterations. Moreover, we found transcriptomic changes in novel molecules that are involved in peripheral neuron–SC interaction.

Keywords Gamma-aminobutyric acid · GABA-A receptor · Peripheral nerve regeneration · Conditional mice

Introduction

Recent evidence shows that the peripheral nervous system (PNS) possess a fully functional γ-aminobutyric acid (GABA) system, consisting in both the neurotransmitter GABA and some of its receptors [1–7]. Indeed, morphological and molecular data gathered from GABA type B1 (GABA-B1) receptor total null mice showed significant alterations in the myelin sheaths, as well as changes in the expression of the peripheral myelin protein-22 (PMP22) and myelin protein zero (P0). These mice have a high percentage of small myelinated fibres and a great number of small dorsal root ganglion (DRG) neurons, which determine altered motor-sensory functions and pain behaviour, such as hyperalgesia, gait abnormalities and motor coordination disturbance [8].

These findings underlined the importance of GABA-B receptors in Schwann cells (SCs), suggesting a role in the control of the myelination process; nevertheless, the involvement of the peripheral neuronal compartment (e.g. small DRG neurons) in determining such changes was not excluded [1, 8]. The study of conditional P0-GABA-B1$^{fl/fl}$ mice, lacking the GABA-B1 receptor specifically in SCs, unravelled this issue. Indeed, P0-GABA-B1$^{fl/fl}$ mice showed a characteristic morphological phenotype, with an increased number of unmyelinated fibres and Remak bundles, including nociceptive C-fibres. The P0-GABA-B1$^{fl/fl}$ mice were hyperalgesic and allodynic; moreover, the morphological and behavioural changes were associated with a downregulation of neuregulin (NRG) 1 expression in peripheral nerves. Therefore, we suggested that the increased pain sensitivity and altered threshold may derive from the loss of GABA-B receptor functions specifically in SCs, and may be the consequence of a preferential SC maturation towards the non-myelinating phenotype [1, 6]. Immunolabelling of GABA-B1 in teased nerve fibres, as well as in SCs and DRG neuronal cultures, further supported the

✉ Valerio Magnaghi
valerio.magnaghi@unimi.it

[1] Blond McIndoe Laboratories, Division of Cell Matrix Biology and Regenerative Medicine, Faculty of Biology, Medicine and Health, The University of Manchester, Manchester, UK

[2] Department of Pharmacological and Biomolecular Sciences, Università degli Studi di Milano, Via G. Balzaretti 9, 20133 Milan, Italy

[3] Computational Biology and Systems Biomedicine, Biodonostia Health Research Institute, San Sebastián, Spain

[4] Ikerbasque, Basque Foundation for Science, Bilbao, Spain

[5] Institute of Biomedical Technologies, National Research Council, Milan, Italy

preferential GABA-B1 localisation in non-myelinating SCs surrounding groups of unmyelinated axons, namely C-fibres [6]. However, the GABA-B receptor subunits, as well as GABA and glutamic acid decarboxylase (GAD) 65/67 enzymes, were also found at the node of Ranvier in a small sub-population of myelinated sensory fibres [9]. Importantly, GABA-B receptor expression, and possibly its activity are upregulated in the SCs of injured nerves. Indeed, their pharmacological inhibition might be part of a process controlling myelin protein expression and re-myelination following the injury [9, 10]. In line with this hypothesis, it is conceivable that the increase in GABA-B receptor expression, found in the SCs of injured nerves, may be part of a physiological response addressed to stimulate the proximal axons to re-grow distally to the injury [9].

Overall, we suggested that GABA-B receptors are important for SC commitment to a non-myelinating phenotype during development. However, P0-GABA-B1$^{fl/fl}$ mice also presented axon modifications, suggesting the presence of SC non-autonomous effects mediated through the neuronal compartment. Interestingly, we hypothesised that a mechanism occurring in the neuronal compartment may concur to the morphological and behavioural phenotype of mice lacking GABA-B1 specifically in SCs.

In this paper, we aim to corroborate previous in vivo observations by studying in vitro primary SC and DRG neuronal cultures obtained from P0-GABA-B1$^{fl/fl}$ (experimental) and GABA-B1$^{fl/fl}$ (control) mice, analysed separately or in co-culture systems. Furthermore, we analysed the transcriptome of pure DRG neuron and SC cultures by Affymetrix GeneChip array. Our results show differences between control and experimental cell cultures in terms of DRG axonal sprouting, SC proliferation, migration and myelination properties. Moreover, we found transcriptomic changes in novel molecules/genes that were not previously associated with peripheral neuron–SC interaction pathways.

Material and Methods

Mice and Genotyping

GABA-B1$^{fl/fl}$ mice [11] were crossed with P0-CRE deleter mice [12] to obtain P0-GABA-B1$^{fl/+}$ mice, which were then back-crossed with GABA-B1$^{fl/fl}$ mice. P0-GABA-B1$^{fl/fl}$ mice, with specific deletion of GABA-B1 in SCs, were chosen as the experimental group and were compared to GABA-B1$^{fl/fl}$ mice chosen as control. Genotyping was performed as previously described [1].

All experiments involving the use of mice SC and neuronal primary cultures were performed in accordance with current Italian and European rules concerning care and use of animals (D.Lvo. n. 26, 4 March 2014; Council Directive 2010/63/EU of the European parliament and the Council of 22 September 2010 on the protection of animal used for scientific purposes) and according to 3R's guidelines. All the experiments were performed according to the guidelines of the Animal Research Committee of the University of Milan.

Cell Cultures

SC and DRG neuronal cultures were obtained from 3-month-old mice, as previously described [1].

SC Cultures Briefly, sciatic nerves from 3-month-old mice were digested with 0.0625% (*w*/*v*) collagenase Type IV (Worthington Biochemical, Lakewood, NJ, USA) and dispase (0.5 mg/ml; Life Technologies Italia) for 45 min, followed by 30 min of 0.25% trypsin (Worthington Biochemical) treatment. Tissue suspension was then mechanically dissociated, filtered through a 100 μm cell sieve (BD Biosciences, San Jose, California, USA) and centrifuged 5 min at 900 rpm. Pellets were suspended and the cell suspension (6×10^4 cells) was seeded on poly-L-lysine (100 μg/ml)–laminin (2 μg/ml) coated 35 mm Petri dishes, in DMEM-FCS 10% plus 2 μM forskolin and 10 pM insulin, at 37 °C, 5% CO_2 and 95% humidity.

DRG Neuronal Cultures Briefly, DRGs were dissociated [13] for 40 min in Ham's F12 medium (Life Technologies Italia), containing 0.125% (*w*/*v*) collagenase Type IV (Worthington Biochemical), followed by 30 min digestion with 0.25% (*w*/*v*) trypsin (Worthington Biochemical) and filtration with 100 μm cell sieve (BD Biosciences). Cells were suspended in Ham's F12 and purified on a gradient of 15% (*w*/*v*) bovine serum albumin (BSA; Sigma-Aldrich, Milan, Italy). The final neuronal pellet was suspended in Bottenstein and Sato's medium with minor changes (BSM—F12 medium plus 1:1 N2 (100 μM putrescine, 30 nM sodium selenite, 20 nM progesterone, 0.1 mg/ml BSA, 1.3 mM transferrin and 10 pM insulin), all Sigma-Aldrich) plus 10 μM arabinoside C (AraC; Sigma-Aldrich). A cell suspension (1.5×10^4) of neurons was seeded on a 35 mm Petri dish coated with poly-L-lysine (100 μg/ml)–laminin (2 μg/ml) (Sigma-Aldrich). After 2 h, nerve growth factor 50 ng/ml was added and cells were grown at 37 °C, 5% CO_2 and 95% humidity.

DRG and SC Co-Culture and In Vitro Myelination

Mice DRG and SC co-cultures were set up on poly-L-lysine (100 μg/ml)–laminin (2 μg/ml) coated Petri dishes as previously described for rat cultures [14] with minor changes. To this end, dissociated DRG neurons were plated on Petri as described above and incubated for 3 days in vitro (div), in presence of 10 μM AraC to avoid endogenous glial cell contamination. In parallel, SCs obtained as described above were

trypsinised, suspended in differentiating co-culture medium (F12 plus DMEM (1:1), FBS 2.5% (*v*/*v*), forskolin 4 μM, 1× N2 complement, NGF 50 ng/ml) and plated (2×10^4 cells/well) on the top of pre-seeded DRG neurons plates. After 5 div, media was switched to myelinating medium: F12 plus DMEM (1:1), FBS 2.5% (*v*/*v*), 1× N2 complement, NGF 50 ng/ml, GGF 126 ng/ml and ascorbic acid 1 mg/ml. Medium was changed every 3 days. Cells were maintained in myelination medium up to 21 days before processing for light microscopy (Axiovert 200; Zeiss, Germany) or immunofluorescence (IFL) analysis.

Proliferation, Migration and Chemotaxis Assay

Proliferation assay on SCs, from experimental or control mice, was performed using an automated cell counter (Luna®; Logos Biosystems Inc., Annandale, USA); 1×10^5 cells were plated into 35 mm Petri dishes and collected after 48 and 72 h with trypsin 0.05%–EDTA 0.02% in phosphate buffer solution (PBS; Euroclone). Cell suspensions were counted with the vital stain Trypan Blue (Logos Biosystems, Annandale, VA, USA); each experimental point was in quadruplicate and experiments replicated at least three times. Wound healing assay was performed by making a scratch on the bottom of the Petri dish, followed by a media change with the addition of mitomycin-C 50 ng/ml (Sigma-Aldrich) to counteract cell proliferation. Cells were then photographed with a scanning microscope (Axiovert 200; Zeiss, Germany) at different time points: 6, 24, 48 and 72 h after the scratch. Pictures were acquired using MetaVue software and the distances between cell fronts were measured with Image-ProPlus 6.0 (Media Cybernetics, Rockville, MD, USA), with at least nine measurements taken from the top to the bottom of the Petri dish. Migration was also tested by Boyden assay (chemotaxis) using a 48-well Boyden's chamber, according to manufacturer's instructions (Neuroprobe, Cabin John, MD, USA). Then 28 μl of control medium (DMEM) or DMEM/FCS 1% was placed in the lower compartment of the chamber, as chemo-attractants. The open-bottom wells of the upper compartment were filled with cells (1×10^5 cells/well), collected by trypsin treatment and suspended in DMEM + 0.1% bovine serum albumin (BSA; Sigma-Aldrich). Cells migrate through a polyvinylpyrrolidone-free polycarbonate porous membrane (8 μm pores) precoated with gelatine (0.2 mg/ml in PBS, 5 days at 4 °C). After migration (overnight, 37 °C, 5% CO_2 and 95% humidity), cells adherent to the underside of the membrane were fixed by methanol and stained according to the Diff-Quik kit (Biomap, Milan, Italy). For quantitative analysis, cells were counted using a ×40 objective on an optical microscope; three random objective fields were counted for each well and the mean number of migrating cells was calculated.

RNA Extraction and qRT-PCR

RNA samples from experimental and control SC and DRG neuronal cultures were extracted using Trizol™ (Gibco-Life Technologies) according to the manufacturer's protocol and quantified with NanoDrop2000 (Thermo Scientific). Pure RNA was obtained after DNAse I treatment with a specific kit (Sigma-Aldrich). One microgram of RNA was reverse-transcribed to cDNA using iScript™ Reverse Transcription Supermix for RT-qPCR (Bio-Rad, Hercules, CA). Primers (see sequences in Table 1) were designed with the PrimerBlast software (NIH, Bethesda, MD, USA).

Ten nanograms of cDNA for each sample were used for real-time PCR. qRT-PCR was performed by measuring the incorporation of SYBR Green dye (Bio-Rad, Italy) on CFX 96 Real Time System-C1000 touch thermal cycler (Bio-Rad). Data analysis was performed using the CFX Manager 2.0 software (Bio-Rad), based on the ΔΔCt method for the relative quantification. The threshold cycle number (Ct) values of both the calibrator and the samples of interest were normalised to the Ct of the endogenous

Table 1 Sequences of primers used in qRT-PCR

Primer name	Primer sequence
RAα2-R	AGACAGGGCCAAAACTGGTCA
RAα3-F	GCTTAGCCTCCAACTTGTTTCTCC
RAα3-R	GAAGAGACCTGTGAGATCGAGTGT
RAα4-F	TCCTGGATTTGGGGGTCCTGTTA
RAα4-R	TCAACATCAGAAACGGGCCCAA
RAα5-F	CCAGTCACTTTGGCTTTTCGCA
RAα5-R	AGGCCGCAGTCTGTTGTCAT
RAβ1-F	TTGGGGCTTCTCTCTTTTCCCG
RAβ1-R	TGCTGGGTTCATTGGAGCTGT
RAβ2-F	TGCTGGGTTCATTGGAGCTGT
RAβ2-R	CGCACGGCGTACCAAAACAT
RAβ3-F	TGTCACTGGCGTGGAAAGGA
RAβ3-R	ATAGGCACCTGTGGCGAAGA
RAγ2-F	CATGGAGCATTGGAAGCTCAGTC
RAγ2-R	TGTGAAGCCTGGGTAGAGCGAT
Raδ-F	TGCCCACTTCAATGCCGACT
Raδ-R	CATCCATCTCTGCCCTTGGCTT
α-Tubulin-F (m + r)	TCGCGCTGTAAGAAGCAACACC
α-Tubulin-R (r)	GGAGATACACTCACGCATGGTTGC
α-Tubulin-R (m)	ATGGAGATGCACTCACGCATGG
β-Actin-F (r)	ACAGCTGAGAGGGAAATCGTGC
β-Actin-R (r)	CCACAGGATTCCATACCCAGGAAG
β2-Microglobulin-F (m)	CCCTGGTCTTTCTGGTGCTTGT
β2-Microglobulin-R (m)	ATGTTCGGCTTCCCATTCTCCG
β2-Microglobulin-F (r)	GCTTGCCATTCAGAAAACTCCCC

housekeeping genes. Data analysis was performed according to the Pfaffl method [15] and results are expressed as relative expression normalised on the geometric mean of a set of housekeeper genes. As a calibrator, we used the RNA obtained from control samples.

qRT-PCR for miR-338-3p and -5p was performed with the same conditions described above, by using miRCURY LNA™ (Exiqon, Euroclone) containing specific primers and the housekeeping probe hsa-103, still based on the ΔΔCt method for the relative quantification.

Immunocytochemistry and Cell Morphology Assessment

Cells were fixed in 4% (*w*/*v*) paraformaldehyde (PFA) and processed for immunostaining. SC purity (more than 98%) was tested with a specific rabbit polyclonal antibody against glycoprotein P0 (Sigma-Genosys), as previously described [16]. Phalloidin–FITC staining of f-actin (1:250, with phalloidin from *Amanita phalloides*, Sigma P2141) was used to reveal the SC cytoskeleton. Slides were incubated overnight at 4 °C in PBS, 0.25% (*w*/*v*) BSA, 0.1% (*v*/*v*) Triton X-100 and the specific primary antibody. Other primary antibodies used in this experiments were the following: 1:200 rabbit polyclonal anti GABA-B1 (antigen TMILSSQQDAAFAFASLAIVFSS; Abcam 68554); 1:500 rabbit polyclonal anti S100 (Dako Z0311); 1:500 rabbit affinity isolated anti-βIII-tubulin (antigen LISKVREEYPDRIMN, Sigma T3952); 1:500 mouse monoclonal purified anti NF200 (clone RMdO20, Sigma N2912); 1:200 chicken polyclonal anti calcitonin gene related peptide (CGRP; Chemicon, AB5705); 1:200 rat monoclonal anti MBP (antigen DENPVV, Millipore MAB386). The following day, the slides were washed twice and incubated 2 h at room temperature with Alexa-488 (green) or Alexa-594 (red) specific secondary antibodies (1:800, Gibco-Life Technologies). After washing, slides were mounted using Vectashield™ (Vector Laboratories, Burlingame, CA, USA) and nuclei stained with 4,6-diamidino-2-phenylindole (Dapi). To ensure specificity, control slides were incubated in solutions lacking primary antibodies. Confocal microscopy was carried out using a Zeiss LSM 510 System (Gottingen, Germany) and images were processed with Image Pro-Plus 6.0 (Media Cybernetics, Bethesda, MA).

For determination of cell morphology, SCs and DRG neurons were treated and fixed as above, then images were blindly analysed with Image J (v1.47f; National Institutes of Health, Bethesda, MD, USA). Cell length, width and axon length were measured and the ratio was calculated as length/width for each cell measured. At least 20 cells were measured for each picture, and 12 pictures were taken for each experimental group (GABA-B1$^{fl/fl}$ vs. P0-GABA-B1$^{fl/fl}$ mice).

Transcriptomic Expression Profile

Transcriptomic expression profile of cell cultures (SCs and DRG neurons) from P0/GABA-B1$^{fl/fl}$ (experimental) or GABA-B1$^{fl/fl}$ (control) mice was analysed by Affymetrix MoGene 2.0 st arrays. To this end, total RNA was extracted from lysed cells in Qiazol lysis reagent using RNeasy minikit (Qiagen) according to the manufacturer's protocol. RNA quantification was performed using NanoVue spectrophotometer (GE Healthcare). Three micrograms of total RNA were treated with DNAse reaction kit (Sigma-Aldrich) to inactivate possible contaminant DNA.

Biotin-labelled cDNA targets were synthesised starting from 200 ng of total RNA. Double-stranded cDNA synthesis and related cRNA was performed with Ambion® WT Expression Kit (Ambion, Austin, TX). With the same kit, the sense strand cDNA was synthesised before being fragmented and labelled with Affymetrix GeneChip® WT Terminal Labeling Kit (Affymetrix, Santa Clara, CA). All steps of the labelling protocol were performed according to manufacturer's instructions.

Targets were diluted in hybridisation buffer at a concentration of 25 ng/μl, denatured at 99 °C for 5 min, incubated at 45 °C for 5 min and centrifuged at maximum speed for 1 min prior to introduction into the GeneChip® cartridge. A single GeneChip® MOUSE Gene 2.0 ST was then hybridised with each biotin-labelled sense target. Hybridisations were performed for 16 h at 45 °C in a rotisserie oven. GeneChip® cartridges were washed and stained with GeneChip® Hybridization, Wash and Stain Kit in the Affymetrix Fluidics Station 450 following the FS450_0002 standard protocol.

GeneChip arrays were scanned using an Affymetrix GeneChip® Scanner3000 7G using default parameters. The normalisation was calculated with the robust multiarray analysis algorithm [17] and data post-processing performed with MatLab. For the molecular signatures enrichment analysis, the molecular signatures were taken from the gene set collection C5 of the version 3.0 of the Molecular Signatures Database (MSigDB) [18]. The significance of the gene set of the different expressed genes was analysed using an enrichment approach based on the hypergeometric distribution. The significance (*p* value) of the gene set enrichment was calculated using the hypergeometric distribution. The multitest effect influence was corrected through controlling the false discovery rate using the Benjamini–Hochberg correction at a significance level $\alpha = 0.05$.

In Silico miR-338 Analysis

Possible miRNA transcript target were predicted by using MyMIR database (http://www.itb.cnr.it/micro/), a system based on integration, filtering and re-ranking of outputs

produced by different miRNA databases (i.e. miRANDA, TargetScan, RNAHybrid). STRING database (https://string-db.org/) was used to obtain a list of Gene Ontology (http://www.pantherdb.org/panther/ontologies.jsp) biological processes (BP) significantly enriched (p value < 0.05) for miR-338-3p targets.

For the analysis, we used the false discovery rate (FDR) adjusted p value to reduce the possibility of false-positive results. The fold enrichment in miR-338-3p was calculated using the formula: fold enrichment $= (m/n)/(M/N)$, where m = genes target in a BP, n = all genes target in the list, M = all genes in a BP and N = all genes in the genome. A fold enrichment greater than 1 (expected value) indicates that the category is over-represented in the input list.

Statistical Analysis

Data were statistically evaluated by GraphPad Prism 4.00 (San Diego, USA). Statistical significance between groups was determined by means of an unpaired Student's t test or one-way ANOVA with Tukey's post-test. Experiments were repeated at least three times. All data were expressed as mean ± standard error of the mean (SEM) of the determinations performed at a significance level $\alpha = 0.05$.

Results

Selection of P0-GABA-B1$^{fl/fl}$ Mice

P0-GABA-B1$^{fl/fl}$ mice with a SC-specific deletion of the GABA-B1 receptor sequence were genotyped, as previously described [1], and used as experimental mice to derive primary cell cultures. Briefly, by using a set of P5/P6 primers, we selected the P0-GABA-B1$^{fl/fl}$ genotype, presenting a specific band of 740 bp, different from *wildtype* allele, showing a band of 530 bp. A PCR with a set of specific primers, recognising the P0-CRE sequence, generated an amplicon of 492 bp for the experimental mice (P0-GABA-B1$^{fl/fl}$); GABA-B1$^{fl/fl}$ mice, in which the 492 bp band was absent, were used as controls (Fig. 1a). To confirm somatic recombination, genomic DNA from liver and sciatic nerve of P0-GABA-B1$^{fl/fl}$ mice were analysed with a P7/P8 primers set. Liver showed a 1.42-kbp band while sciatic nerve showed a 360-bp band, resulting from the excision of the GABA-B floxed fragment specifically in the sciatic nerve (Fig. 1a). Cells were compared to cultures obtained from GABA-B1$^{fl/fl}$, used as controls.

SCs of P0-GABA-B1$^{fl/fl}$ Mice Express Typical Markers But Not GABA-B1 Receptor

SCs obtained from control and experimental mice were cultured, showing typical in vitro morphology (Fig. 1b). As

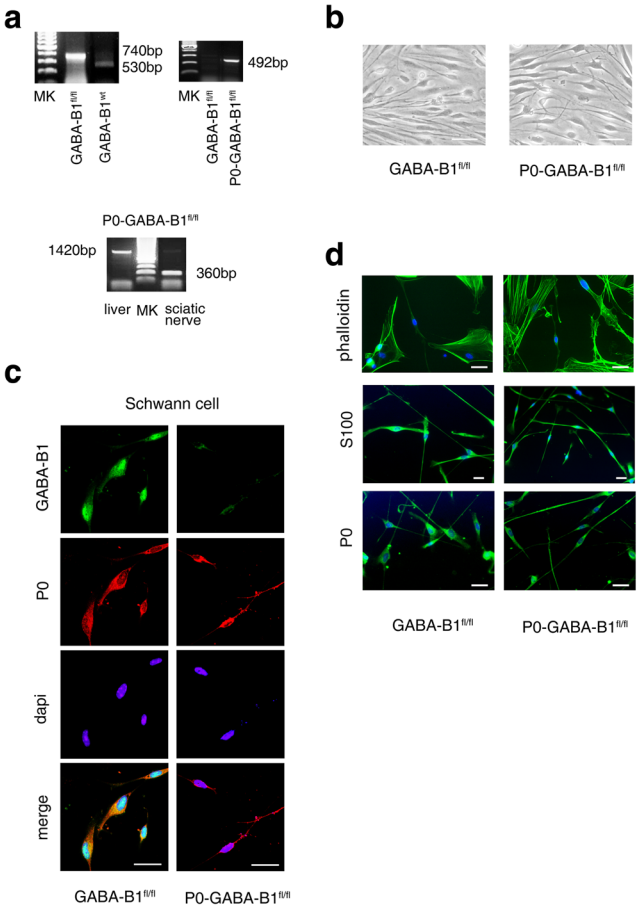

Fig. 1 Characterisation of SCs of P0-GABA-B1$^{fl/fl}$ mice. **a** PCR images of genotyping with CRE1/CRE2, P5/P6 and P7/P8 primers. P5/P6 distinguished the GABA-B1$^{fl/fl}$ (740 bp specific band) from the GABA-B^{wt} genotype (530 bp specific band). CRE1/CRE2 distinguished the P0-GABA-B1$^{fl/fl}$ experimental mice (492 bp band) from GABA-B1$^{fl/fl}$ control mice (band was absent). P7/P8 confirmed P0-GABA-B1$^{fl/fl}$ experimental mice (360 bp band) resulting from the GABA-B floxed fragment in the sciatic nerve, whereas the liver showed a 1420 bp band. **b** Light microscopy images of SCs from P0-GABA-B1$^{fl/fl}$ and GABA-B1$^{fl/fl}$ mice. Bar 10 μm. **c** Immunofluorescence localisation of GABA-B1 (green) in SCs, identified with the specific marker P0 (red). Nuclei stained with dapi (blue). Merged images confirmed the presence of GABA-B1 in SCs from GABA-B1$^{fl/fl}$ and the absence in SCs from P0-GABA-B1$^{fl/fl}$ mice. Scale bar 10 μm. **d** Immunofluorescence images of SCs stained with phalloidin (cytoskeleton marker), S100 and P0 (typical SCs markers) showing that there are no differences between cells from P0-GABA-B1$^{fl/fl}$ and GABA-B1$^{fl/fl}$ mice. Bar 10 μm

expected, the GABA-B1 was absent in SCs from P0-GABA-B1$^{fl/fl}$ mice, although these cells were immunopositive for the most characteristic marker glycoprotein P0 (Fig. 1c). Cell purity was stated about 96–98%. As shown in Fig. 1d, SCs were also immunopositive for S100, another characteristic SC marker. No morphological differences were found between SCs from P0-CRE/GABA-B1$^{fl/fl}$ (experimental) or GABA-B1$^{fl/fl}$ (control) mice. This was confirmed by phalloidin labelling, suggesting no remarkable differences in cytoskeletal structure. The successful establishment of SC cultures from experimental mice and the

immunopositivity for specific markers suggested that SCs are capable of proliferating/differentiating in vitro, regardless of the absence of GABA-B1 receptors.

DRG Neurons of P0-GABA-B1$^{fl/fl}$ Mice Express Normal Neuronal Markers

DRG neuronal cultures were successfully obtained from experimental P0-GABA-B1$^{fl/fl}$ mice and light microscopy observations showed the typical DRG neuron morphology in vitro, with successful attachment and neurites sprouting (Fig. 2a). Given these cells are very sensitive to in vitro culturing, this confirms the reliability of the methodological procedure. Differently from SC cultures (which lacked GABA-B1 receptor immunopositivity), the GABA-B1 receptor was found in DRG from both P0-GABA-B1$^{fl/fl}$ (experimental) and GABA-B1$^{fl/fl}$ (control) mice, as shown by immunofluorescence analysis (Fig. 2b). Moreover, DRG neurons were immunopositive for S-100, high-density neurofilament NF200 and CGRP, the latter one being a marker of peripheral afferents and sensitive neurons (Fig. 2c). As *per* SC cultures, also for DRG neurons, no major morphological differences between cells from P0-GABA-B1$^{fl/fl}$ (experimental) or GABA-B1$^{fl/fl}$ (control) mice were found. Importantly, not all neurons resulted immunolabelled for CGRP, according to a specific labelling for nociceptive fibres as shown also in vivo [19]. However, to investigate further on the functional differences between experimental and control DRG neurons in vitro, we tested the cells for neurites outgrowth by measuring the length of the neuritis using a mouse anti-βIII-tubulin antibody. The average neurite length was significantly reduced ($p < 0.05$) in DRG neurons derived from mice with conditional deletion of the GABA-B1 receptor in SC (Fig. 2d), changing from 305.1 ± 41.28 μm in control cells to 204.2 ± 15.76 μm in experimental cells.

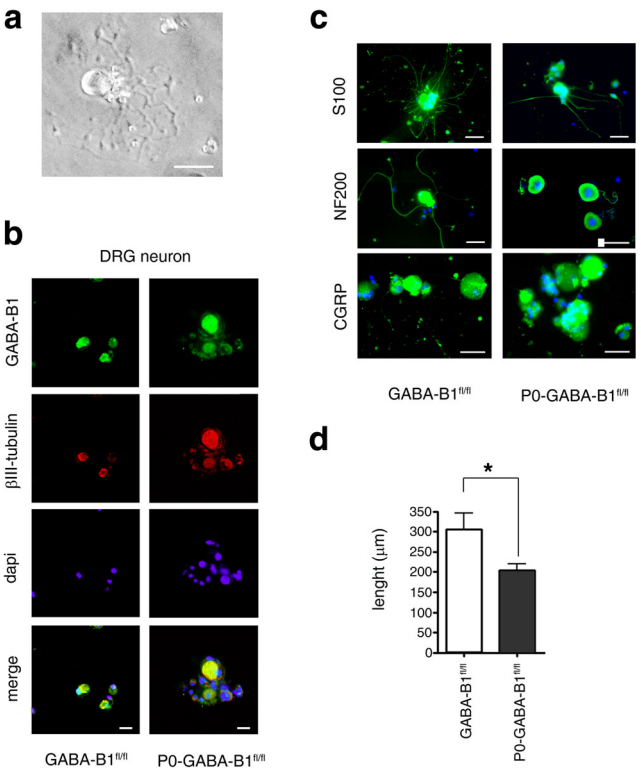

Fig. 2 Characterisation of DRG neurons of P0-GABA-B1$^{fl/fl}$ mice. **a** Light microscopy image of DRG neuron from P0-GABA-B1$^{fl/fl}$ mice. Bar 10 μm. **b** Immunofluorescence localisation of GABA-B1 (green) in DRG neurons, identified with the specific marker βIII-tubulin (red). Nuclei stained with dapi (blue). Merged images confirmed the presence of GABA-B1 in DRG neuron both from GABA-B1$^{fl/fl}$ and P0-GABA-B1$^{fl/fl}$ mice. Scale bar 10 μm. **c** Immunofluorescence images of DRG neurons stained with S100, NF200 and CGRP (characteristic markers) showing that there are no significant differences between cells from P0-GABA-B1$^{fl/fl}$ and GABA-B1$^{fl/fl}$ mice. Bar 10 μm. **d** Assessment of neurites outgrowth (length in μm) by using a mouse anti-βIII-tubulin antibody. Average neurite length was significantly reduced ($p < 0.05$) in DRG neurons from P0-GABA-B1$^{fl/fl}$ mice. Values are means ± SEM ($n = 6$)

SCs of P0-GABA-B1$^{fl/fl}$ Mice Altered Proliferative, Migratory and Myelinating Capacities

We hypothesised that SCs from P0-GABA-B1$^{fl/fl}$ mice, which showed normal morphology, should also preserve proliferative characteristic. To test this hypothesis, we quantified the amount of proliferating SCs in vitro by phase-contrast and immunofluorescence microscopy (against P0 marker) in presence of different concentrations of the mitogen factor forskolin (2, 4 and 100 μM). By qualitative assessment of cell numbers, it was apparent that SCs from P0-GABA-B1$^{fl/fl}$ (experimental) showed a dose-dependent rise in proliferation following exposure to increasing forskolin concentrations (Fig. 3a). Indeed, SCs exposed to high 100 μM forskolin for 14 days showed almost double proliferative capacity, compared to lower forskolin concentrations, 2 and 4 μM (Fig. 3a). Conversely, the quantitative evaluation of SCs from P0-GABA-B1$^{fl/fl}$ mice showed a significant ($p < 0.001$) decrease in proliferation, when exposed for 48 and 72 h to either 4 or 100 μM forskolin (Fig. 3b). Notably, P0-GABA-B1$^{fl/fl}$ experimental mice did not show any significant change between 4 and 100 μM forskolin treatments (Fig. 3b).

In accordance with the literature [20], increases in forskolin concentration changed the morphological parameters of SCs, becoming increasingly spindle-shaped and elongated (differentiated) at higher forskolin concentrations (Fig. 3c). However, quantitative evaluation of SCs aspect ratio, exposed to 100 μm forskolin, did not show any significant change between control and P0-GABA-B1$^{fl/fl}$ experimental cells (Fig. 3c).

Overall, our results corroborate the hypothesis, previously investigated in vivo [1], that GABA-B1 receptors participate

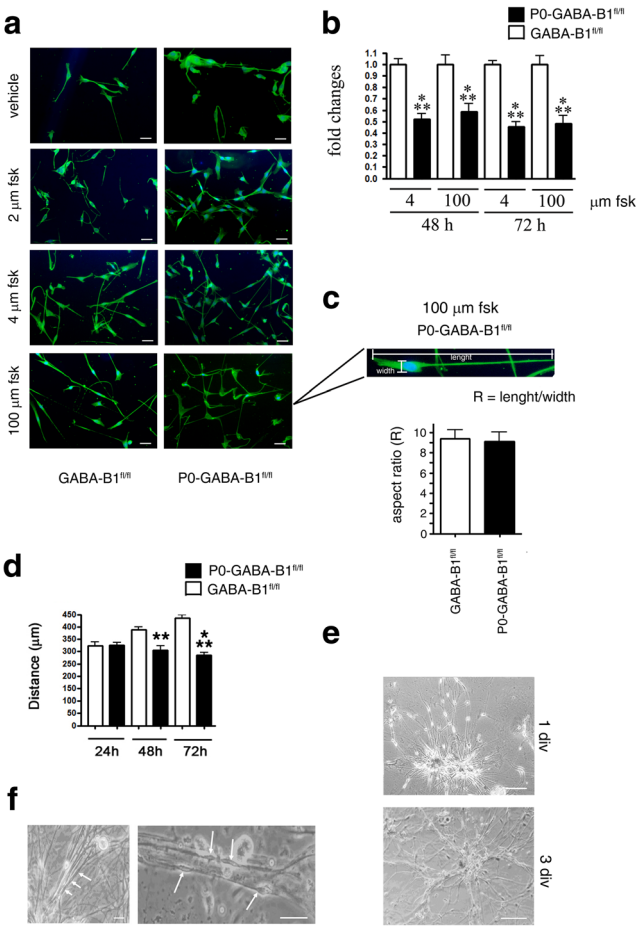

Fig. 3 Proliferative and migratory changes in SCs of P0-GABA-B1$^{fl/fl}$ mice. **a** Immunofluorescence images of SCs, from P0-GABA-B1$^{fl/fl}$ and GABA-B1$^{fl/fl}$ mice, exposed for 14 days to different forskolin (fsk) concentrations (2, 4 and 100 μM) and labelled with an antibody against P0 (green). Bar 10 μm. **b** SCs proliferation was assessed at 48 and 72 h following treatment with 4 and 100 μM fsk, respectively. A significant proliferation decrease was observed with all experimental conditions ($p < 0.001$). Data are expressed as mean of fold changes ± SEM. **c** Magnification of a representative SC elongation in a immunofluorescence image. Aspect ratio was measured in SCs exposed to 100 μM fsk. No significant change between control GABA-B1$^{fl/fl}$ (white column) and P0-GABA-B1$^{fl/fl}$ (black column) experimental cells was observed. **d** Histograms of cell distance (μm) of SCs from P0-GABA-B1$^{fl/fl}$ (black column) and GABA-B1$^{fl/fl}$ (white column) at 24, 48 and 72 h after the scratch. P0-GABA-B1$^{fl/fl}$ experimental mice showed a significant decrease in migratory capability at 48 h ($p < 0.01$) and 72 h ($p < 0.001$). Data are expressed as mean ± SEM. **e** Light microscopy image of DRG neuron and SCs co-culture at 1 day in vitro (div) and 3 div under basal (non-myelinating state) condition. Bar 50 μm. After 7–10 div in basal co-culture conditions, some SCs were aligned alongside neurites (white arrows in **f**, bar 20 μm)

as regulator of SC proliferation. Furthermore, to evaluate the effect of GABA-B1 depletion on functional parameters of SCs, their migratory capability was assessed through a wound healing assay in presence of mitomycin-C 50 ng/ml to block cell proliferation; cells were studied at different time points (24, 48 and 72 h) after the scratch. SCs from P0-GABA-B1$^{fl/fl}$ experimental mice showed a significant decrease in migratory capability at 48 h ($p < 0.01$) and 72 h ($p < 0.001$) after the scratch (Fig. 3d); the distance changed from 387.5 ± 11.21 μm in control to 305.9 ± 17.74 μm in experimental cells after 48 h and from 436.8 ± 12.74 μm in control to 285.9 ± 10.42 μm in experimental cells at the 72-h time point (Fig. 3d).

To evaluate the myelinating capability, which is a key functional output of SCs, we established a co-culture system of SCs with DRG neurons [14]. This is a reliable method that allows fine manipulation of the microenvironment, together with the modelling and studying of the signalling mechanisms between PNS cells. Namely, this in vitro system provides a physiological model for in vivo-like studies of nerve functions. The morphology of the co-culture system with control cells (from GABA-B1$^{fl/fl}$ mice) under basal condition (non-myelinating state) showed that SCs lie underneath and surround DRG neurons, which showed a classic neurites arborisation (Fig. 3e), confirming the good quality of our co-culture system. In particular, after 7–10 days in basal co-culture conditions, some SCs were aligned alongside neurites (white arrows in Fig. 3f), a pre-requisite to start the myelination programme. Myelination was induced with the myelinating medium containing F12 plus DMEM (1:1), FBS 2.5%, N2 complement, forskolin 4 μM, NGF 50 ng/ml, GGF 126 ng/ml and ascorbic acid 1 mg/ml. The co-cultures were stimulated for myelination for 14–21 days, then immunolabelled with anti-βIII-tubulin antibody (neuronal marker) or anti-myelin basic protein (MBP; SCs marker) antibody. As shown in Fig. 4a, SCs in co-culture stained positively for MBP (green), which co-localised with βIII-tubulin (red), producing a merged (yellow) signal. This resembles the myelination process in vitro, peaking around the third week in culture (21st div). The experimental design consisted in crossing the DRG neurons, from P0-GABA-B1$^{fl/fl}$ (experimental) or GABA-B1$^{fl/fl}$ (control) mice, with the SCs from P0-GABA-B1$^{fl/fl}$ (experimental) or GABA-B1$^{fl/fl}$ (control) mice. Therefore, four different conditions were obtained: DRG neurons control with SCs control; DRG neurons experimental with SCs control; DRG neurons control with SCs experimental; DRG neurons experimental with SCs experimental. Treatment of DRG neurons with Ara-C was used prior to co-culture, to prevent any cross-contamination with SCs from the same mice genotype. Cells were then processed for immunofluorescence with a primary antibody against βIII-tubulin (to label neurons) and MBP, to label SCs and myelin (Fig. 4b). The co-culture from control DRG neurons and SCs showed a good grade of myelination, as represented by the merged staining (yellow). Myelination decreased progressively when either control SC or control DRG neurons were replaced with cultures obtained from experimental mice. Interestingly, the lowest amount of myelin staining was found in the co-culture obtained by experimental DRG neurons and experimental SCs (Fig. 4b). Altogether, these findings corroborate

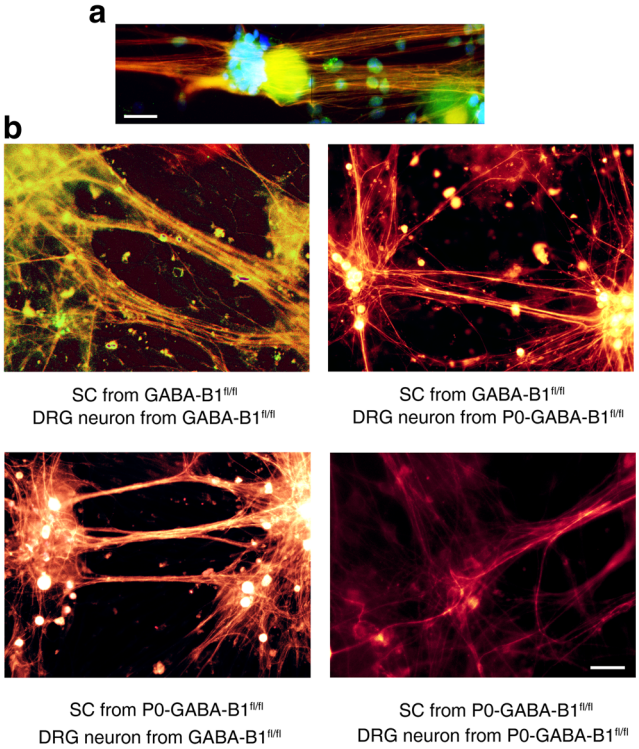

Fig. 4 Changes in an in vitro myelination system of SCs and DRG neurons of P0-GABA-B1$^{fl/fl}$ mice**. a** Immunofluorescence images of SCs and DRG co-culture system of GABA-B1$^{fl/fl}$ mice, mimicking in vitro the myelination process in vivo. SCs stained positively for the specific marker MBP (green), which co-localised with βIII-tubulin marker of neurons (red), producing a merged (yellow) signal. Bar 20 μm. **b** Immunofluorescence images of co-culture. DRG neurons from P0-GABA-B1$^{fl/fl}$ (experimental) or GABA-B1$^{fl/fl}$ (control) mice were crossed with SCs from P0-GABA-B1$^{fl/fl}$ (experimental) or GABA-B1$^{fl/fl}$ (control) mice, obtaining four different experimental conditions. SCs marker MBP in green and neuron βIII-tubulin marker in red; merge in yellow. Myelination decreased progressively when either control SC or control DRG neurons were replaced with cells from experimental mice. Bar 20 μm

our previous results in vivo, supporting the role of GABA-B1 receptor in controlling the peripheral myelination process. Indeed, as expected in the co-culture obtained from both DRG neurons and SCs originated from GABA-B1-deficient mice, the myelination process resulted in a strongly compromised state also in vitro (Fig. 4b). These findings further support the importance of the peripheral cross-talk between neuronal and glial cells for a key process such as myelination.

Identification of Target Genes in SCs and DRG Neurons of P0-GABA-B1$^{fl/fl}$ Mice by Genome-Wide Screening

We then further investigated GABA-B1 receptor function by evaluating the transcriptomic expression profile of SCs and DRG neurons from P0-GABA-B1$^{fl/fl}$ (experimental) or GABA-B1$^{fl/fl}$ (control) mice. The results obtained showed a considerable amount of genes modulated in both SC and DRG neuron by the selective deletion of the GABA-B1 receptor in SCs, thus supporting the importance of the cross-talk, and the presence of SC non-autonomous effects downstream GABA-B1 activation in vitro.

In SCs, we found expression changes of several genes encoding for distinct classes of proteins involved in several intracellular pathways relevant for neuroinflammation, adhesion and cell proliferation (i.e. cytokines, chemokines or proteins of the extracellular matrix, etc.). From the total number of transcripts in the microarrays (41,345), we found 1099 transcripts, accounting for 2.66% of total transcripts, differentially expressed in control versus experimental SCs. The first set of 276 genes, with an expression level log-2 scaled, were differentially expressed in P0-GABA-B1$^{fl/fl}$ mice; we found 38 downregulated and 238 upregulated genes in P0-GABA-B1$^{fl/fl}$ mice versus controls (Fig. 5a). The molecular signatures enrichment analysis discloses that some of these genes modulate common intracellular mechanisms, regulating similar physiological functions. As shown in Fig. 5b, most of the upregulated proteins belong to the extracellular matrix, supporting our findings on altered migration capability of SCs and confirming the relevance of GABA-B1 receptor in controlling SC plasticity. Furthermore, several families of chemokines and cytokines genes were found to be upregulated in P0-GABA-B1$^{fl/fl}$, stressing the putative role of GABA-B1 receptor in the neuroinflammatory response and in peripheral nociceptive processes.

The heat map (Fig. 5c) was calculated based on the criteria of the *p* value and 1 log2-fold change, and showed the following top upregulated genes: *Gzme*, *Mmp3*, *Tfpi2*, *Fgf7*, *Serpinb2*, *Pcdh19*, *Osr1* and *Vcan.*

The analysis of the DRG neurons transcriptome also suggested some changes in the expression of genes coding for proteins controlling key cellular pathways. Among 41,345 transcripts in the microarrays, 1.85% of total genes (corresponding to 764 genes) were differently expressed. The first set of 59 genes, with an expression level log-2 scaled, were differently expressed in P0-GABA-B1$^{fl/fl}$ mice; 33 genes were downregulated while 26 upregulated genes in P0-GABA-B1$^{fl/fl}$ mice (Fig. 5d). Almost the entirety of these genes was related to synaptic transmission, acetylcholine transmission and to the nicotinic gated receptors family (Fig. 5e).

miR-338 Is Modulated in SCs of P0-GABA-B1$^{fl/fl}$ Mice: qRT-PCR and In Silico Analysis

Interestingly, transcriptomic analysis showed that some miRNAs were up- or downregulated in P0-GABA-B1$^{fl/fl}$ mice. We focused our attention on miR-338, which has been implicated in oligodendrocyte maturation and mainly in SC differentiation [21, 22]. First, we confirmed miR-338 expression in SCs cultures from both P0-GABA-B1$^{fl/fl}$ and GABA-B1$^{fl/fl}$ mice, finding a significant downregulation ($p < 0.01$) of the

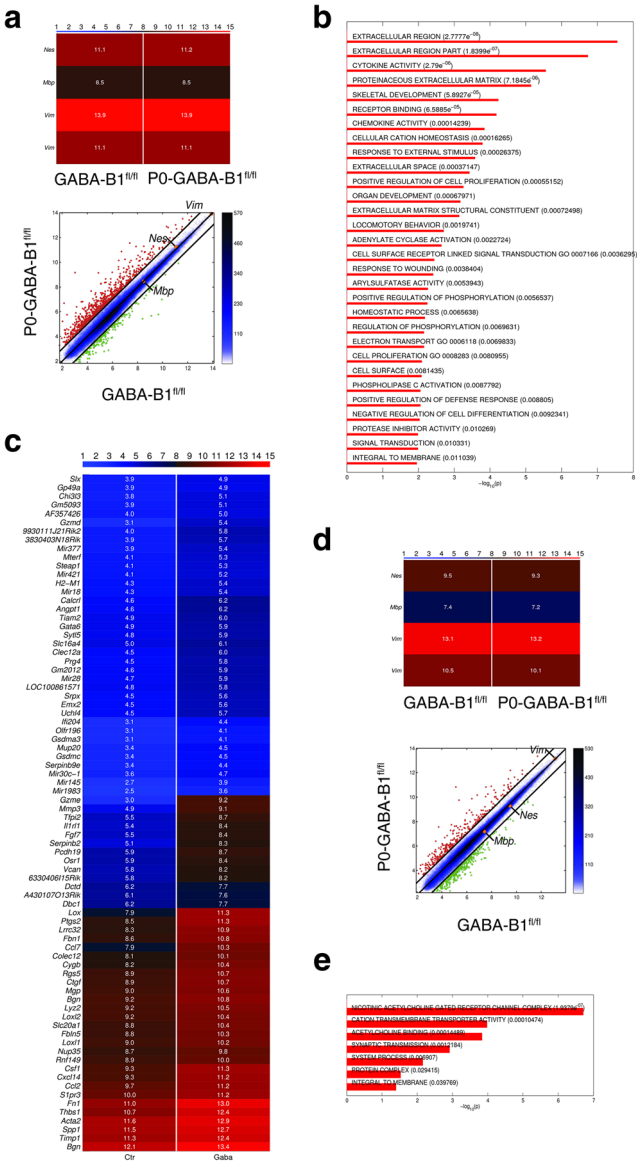

Fig. 5 Genome-wide screening identification of target genes in SCs and DRG neurons of P0-GABA-B1$^{fl/fl}$ mice. **a** Pairwise scatter plot of SC from GABA-B1$^{fl/fl}$ (control) versus P0-GABA-B1$^{fl/fl}$ (experimental) mice. The heat map on top shows the expression of all the probes associated with the genes appearing in scatter plots. The colour bar in the top codifies the gene expression in log2 scale. The higher is the gene expression the more red is the colour. **b** Plot bar of the − log10(*p*) of the significant enriched terms of SC from GABA-B1$^{fl/fl}$ (control) versus P0-GABA-B1$^{fl/fl}$ (experimental) mice − log2(2). The longer the bar, the higher is the statistical significance of the enrichment (*p* values in parentheses). **c** Heat map of the top upregulated genes in SC from GABA-B1$^{fl/fl}$ (control) versus P0-GABA-B1$^{fl/fl}$ (experimental) mice. **d** Pairwise scatter plot of DRG neurons from GABA-B1$^{fl/fl}$ (control) versus P0-GABA-B1$^{fl/fl}$ (experimental) mice. The heat map on top shows the expression of all the probes associated with the genes appearing in scatter plots. The colour bar in the top codifies the gene expression in log2 scale. The higher the gene expression, the more intense the red colour. **e** Plot bar of the − log10(*p*) of the significant enriched terms of DRG neurons from GABA-B1$^{fl/fl}$ (control) versus P0-GABA-B1$^{fl/fl}$ (experimental) mice − log2(2). The longer the bar, the higher is the statistical significance of the enrichment (*p* values in parentheses)

miR-338 3p segment (miR-338-3p) (Fig. 6a), while the 5p segment did not change (Fig. 6b). Then, to investigate the potential role of miR-338-3p in our model, we performed in silico analysis on the mouse MyMIR databases. We obtained a list of 729 putative target transcripts of miR-338-3p in mouse. Thereafter, we used STRING, a Gene Ontology (GO) based tool, finding that these targets were significantly clustered in three principal pathways: biological processes, molecular functions and cellular compartment; this suggested that miR-338-3p takes part in their regulation. Then we focused on 'biological processes', calculating the fold enrichment in miR-338-3p target transcripts in the different sub-pathways, using the following equation:

$$\text{Fold enrichment} = \frac{m \div n}{M \div N}$$

where '*m*' are the target genes in 'biological processes'; '*n*' are all genes in the list; '*M*' are all genes in 'biological processes'; '*N*' are all genes in the genome.

Based on the fold enrichment and *p* value (of the false discovery rate, FDR), the main GO biological pathways involved are nervous system development, anatomical structure morphogenesis, signal transduction, intracellular signalling transduction, synaptic transmission and cell-to-cell signalling (Fig. 6c).

GABA-A Receptor Subunits Are Cross-Modulated in P0-GABA-B1$^{fl/fl}$ Mice

The peripheral GABAergic system also includes GABA-A receptors. Thus, it was of interest to analyse the basal GABA-A receptor subunit expression in SCs and DRG neurons. We focused the attention on classic subunits (e.g. α2, α3, β1–3, γ2) and also on subunits commonly forming the extra-synaptic receptors (e.g. α4, α5 and δ), which are attracting increasing interest in recent years [23, 24]; these subunits have not been previously characterised in the PNS. Performing this analysis, we confirmed that synaptic subunits (e.g. α2, α3, β1, β2, β3 and γ2) are expressed in SCs [25]; interestingly, also the extra-synaptic α4, α5 and δ receptor subunits were found in SCs (Fig. 7a, left panel). Similarly, all synaptic and extra-synaptic subunits were also found in DRG neurons (Fig. 7a, right panel). Basal expression in SCs showed a prevalence of extra-synaptic-like GABA-A subunits (e.g. α4 and δ subunits, alongside the β3 subunit). Indeed, DRG neurons showed higher expression of synaptic GABA-A subunits, including the characteristic α2 and γ2 subunits, and of the β3 subunit (Fig. 7a).

Then, we analysed whether depletion of GABA-B1 receptor in P0-GABA-B1$^{fl/fl}$ mice resulted into a cross-regulation of GABA-A receptors.

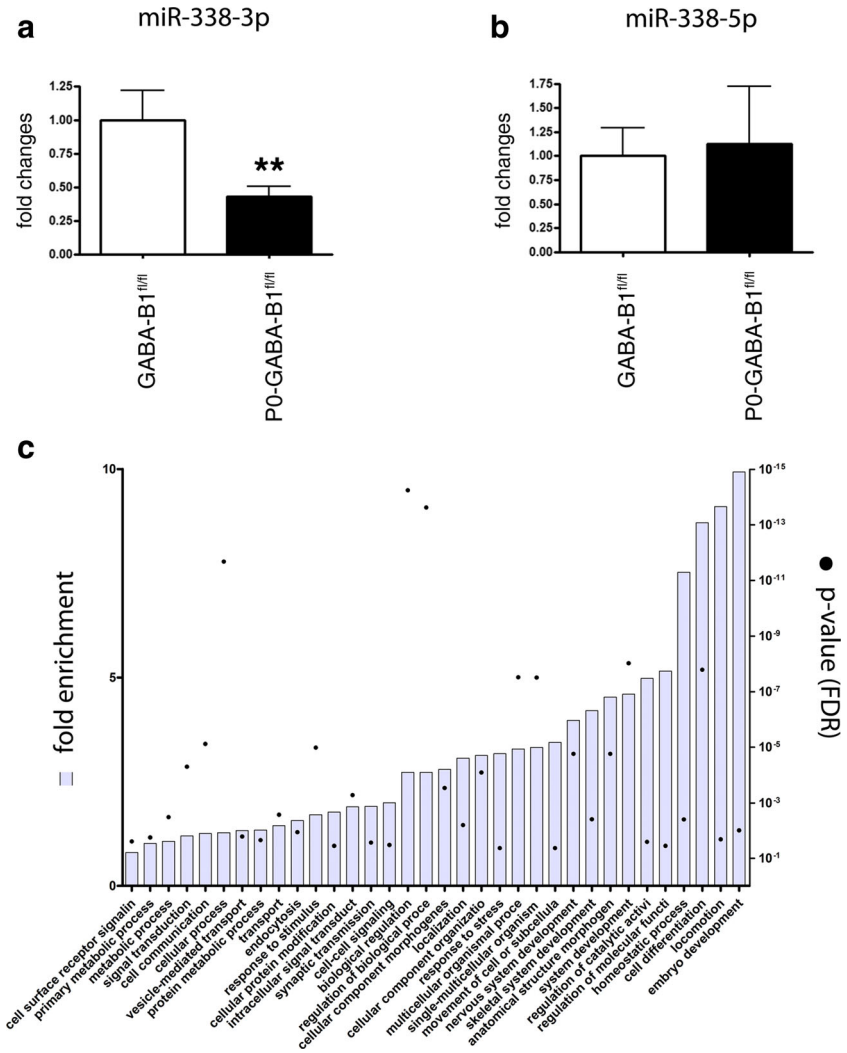

Fig. 6 qRT-PCR and in silico analysis of miR-338 in SCs of P0-GABA-B1$^{fl/fl}$ mice. **a** qRT-PCR of mRNA levels (expressed as fold changes), coding for miR-338-3p showed a decreased expression in P0-GABA-B1$^{fl/fl}$ mice (black column). Data were normalised to the housekeeping gene hsa-103 and expressed as difference ($\Delta\Delta$Ct) versus GABA-B1$^{fl/fl}$ (control, white column). Values are means ± SEM ($n = 10$); $^{**}p < 0.01$. **b** qRT-PCR of mRNA levels (expressed as fold changes), coding for miR-338-5p. Data were normalised to the housekeeping gene hsa-103 and expressed as difference ($\Delta\Delta$Ct) versus GABA-B1$^{fl/fl}$ (control, white column). Values are means ± SEM ($N = 10$). **c** Gene Ontology biological processes (GO BPs) related to SCs development are enriched in miR-338-3p targets. Histograms show the significant GO BPs enriched in miR-338-3p target transcripts (fold enrichment compared to expected value = 1; left axis). Dots represent p value (with FDR correction) of the prediction for each GO BP (right axis; log10 scale)

Quantitative analysis by qRT-PCR showed a clear tendency towards downregulation of some subunits in both SCs and DRG neurons (Fig. 7b, c) in (experimental) P0-GABA-B1$^{fl/fl}$ compared to GABA-B1$^{fl/fl}$ (control) mice. In particular, the α3 subunit was significantly downregulated in both SCs ($p < 0.05$) and DRG neurons ($p < 0.01$) of GABA-B1$^{fl/fl}$ experimental mice, compared to P0-GABA-B1$^{fl/fl}$ controls. Additionally, α4 ($p < 0.05$), β1 ($p < 0.001$) and δ ($p < 0.01$) were significantly downregulated in DRG neurons of P0-GABA-B1$^{fl/fl}$ (experimental) mice, suggesting a neuron-specific control of extra-synaptic GABA-subunits in P0-GABA-B1$^{fl/fl}$ mice. Overall, other GABA-A subunits seemed to be unaltered in the experimental mice versus control.

Discussion

In this study, we investigated in vitro primary cultures (isolated or in a co-culture system) of SCs and DRG neurons from P0/GABA-B1$^{fl/fl}$ mice, finding proliferative, migratory and myelinating modifications, as well as molecular and transcriptomic changes, that corroborate our previous data on the role of GABA-B1 receptor in the peripheral neuron–SC cross-talk during development and maturation.

A recent in vivo study of P0-GABA-B1$^{fl/fl}$ conditional mice [1] showed a characteristic morphological phenotype, with increased number of small unmyelinated fibres and Remak bundles, including nociceptive C-fibres, thereby pointing to a role of GABA-B receptors in the regulation of non-myelinating SCs and nociceptive pathways in the PNS. Discerning the role of GABA-B receptors in SCs and DRG neurons may be important to understand glial or neuronal-mediated mechanisms and may be relevant for the management of peripheral neuropathies and associated pain.

For instance, the decrease in neurite length in cultured DRG neurons from P0-GABA-B1$^{fl/fl}$ conditional mice proved that the GABA-B1 receptor in the PNS may exert a double control: it may directly regulate SCs during development, and contemporarily it may indirectly regulate DRG neurons

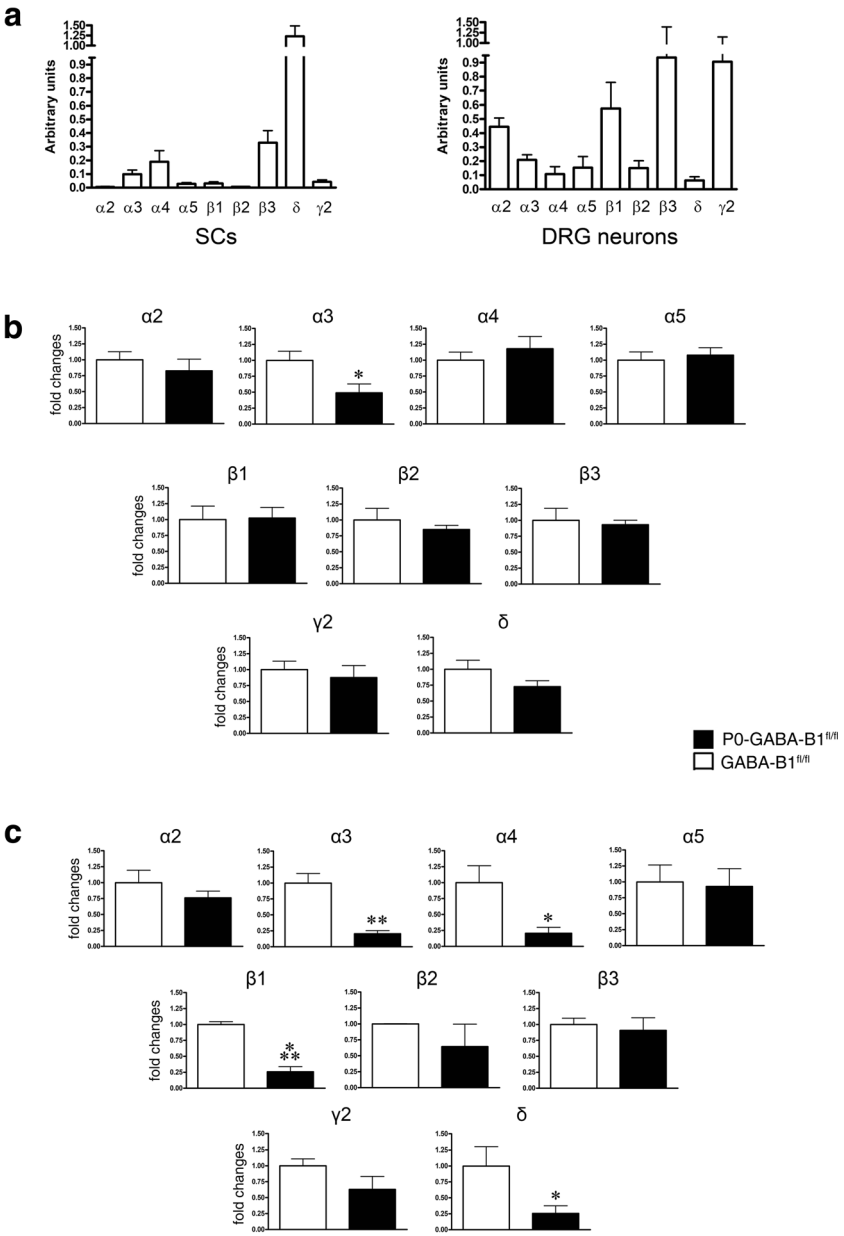

Fig. 7 GABA-A receptor subunits are cross-modulated in P0-GABA-B1$^{fl/fl}$ mice. **a** qRT-PCR analysis of basal GABA-A receptor subunits expression in SCs and DRG neurons. Basal SCs showed a prevalent expression of extra-synaptic-like GABA-A subunits, while DRG neurons showed higher synaptic types. Values are mean ± SEM ($N = 6$). **b** qRT-PCR analysis of relative mRNA levels (expressed as fold changes) coding for α2, α3, α4, α5, β1, β2, β3, δ and γ2 subunits of GABA-A receptor in SCs of P0-GABA-B1$^{fl/fl}$ mice (black column) versus GABA-B1$^{fl/fl}$ (control, white column). Values are means ± SEM ($N = 10$); * $p < 0.05$. **c** qRT-PCR analysis of relative mRNA levels (expressed as fold changes) coding for α2, α3, α4, α5, β1, β2, β3, δ and γ2 subunits of GABA-A receptor in DRG neurons of P0-GABA-B1$^{fl/fl}$ mice (black column) versus GABA-B1$^{fl/fl}$ (control, white column). Values are means ± SEM ($N = 10$); *$p < 0.05$, **$p < 0.01$, ***$p < 0.001$

morphology, at least in vitro. This outcome corroborates our hypothesis on a GABA-B-mediated cross-control of SCs and DRG neurons. In this scenario, DRG cultures obtained by P0-GABA-B1$^{fl/fl}$ conditional mice, albeit genetically identical to GABA-B1$^{fl/fl}$ (both still expressing GABA-B1), showed physiological differences (such as altered neurite length, reduced myelination capacity and other molecular features), which might be ascribed to the cross-talk with P0-GABA-B1$^{fl/fl}$ SC during PNS development. It is worth mentioning that control DRG (GABA-B1$^{fl/fl}$) should have the same characteristic of experimental DRG (P0-GABA-B1$^{fl/fl}$), whereas the latter seemed to perform worse than control DRGs. During development, indeed, the lack of GABA-B1 likely made DRG neurons less prone to be myelinated by SCs.

Moreover, SCs of P0-GABA-B1$^{fl/fl}$ mice showed altered proliferative, migratory and myelinating capacities. Indeed, independently by the presence of GABA-B1, SCs proliferate in presence of increasing forskolin concentrations (from 2 to 100 μM). It is generally known that forskolin acts as a proliferative factor in SCs, rising intracellular 3′,5′-cyclic adenosine monophosphate (cAMP) levels, in turn inducing cell proliferation [26, 27]. However, the P0-GABA-B1$^{fl/fl}$ mice showed a decreased proliferative and migratory capacities, suggesting that GABA-B1 receptor participates in regulating these properties. Importantly, co-culture experiments demonstrated that cells derived from the P0-GABA-B1$^{fl/fl}$ mice have an altered myelinating potentiality; SCs presented lower myelinating capability, while DRG neurons showed altered myelinating

'receptivity' in the experimental groups compared to controls. In agreement with our previous in vivo data [1], these findings corroborate the hypothesis that GABA-B1 receptor participates in the regulation of SCs differentiation and plasticity towards the non-myelinating state.

Changes in SCs transcriptomic patterns might be in agreement with the biochemical outcomes observed. Indeed, some of the genes upregulated in P0-GABA-B1$^{fl/fl}$ mice (i.e. *Gzme*, *Mmp3*, *Tfpi2*, *Fgf7*, *Serpinb2*, *Pcdh19*, *Osr1*, *Vcan*) are involved in differentiation or proliferation/migration of different cell types and tissues. For instance, *Vcan* is a gene related to system development, which regulates the early stage of neural stem cell differentiation, through WNT/beta-catenin, into astrocytes [28]; Vcan encodes for the protein versican, an extracellular matrix component. Up-regulation of versican has been correlated to an adhesion inhibition of neonatal DRG neurons and SCs in vitro [29]. Furthermore Mmp3 encodes for the matrix metalloproteinases 3, which is a key regulator of the extracellular matrix, playing a structural role in maintaining the spatial relationship between muscle cell, SCs and presynaptic motor neurons [30]. Interestingly, the *Fgf7* gene, encoding for the fibroblast growth factor 7 (FGF7), seems to be involved in promoting the organisation of excitatory and inhibitory presynaptic terminals in the hippocampus [31]. Mice lacking FGF7 are prone to epileptic seizures [31], whereas the correlation of FGF7 levels with GABA receptor in the PNS is mostly unknown.

Microarray analysis on SCs of P0-GABA-B1$^{fl/fl}$ also found changes in a series of miRNAs, which are usually developmentally regulated during SC maturation and myelination [21, 32–34]. Among these we focused on miR-338, which is implicated in SC differentiation [21, 22]. miR-338, at least the segment 3p, was decreased in SCs of P0-GABA-B1$^{fl/fl}$. Notably, some miRNAs rise in pre-myelinating SCs, but drop down during myelination [35]. In this light, the decrease in miR-338-3p was in accordance with the loss of myelinating capacity showed by the SC-DRG P0-GABA-B1$^{fl/fl}$ co-culture system.

Interestingly, in this study, we confirmed the expression of some GABA-A receptor subunits (synaptic and extra-synaptic) in both neuronal and glial compartment, and detected the expression of GABA-A subunits that have not been previously identified in the PNS. Moreover, the expression levels of these GABA-A receptor subunits are cross-modulated in SCs and DRG neurons from P0-GABA-B1$^{fl/fl}$ mice. The basal expression level of some GABA-A subunits has been previously investigated in rat sciatic nerves and SCs, suggesting for example that α1 and α6 subunits are not importantly expressed in peripheral nerves [36]. However, extra-synaptic subunit expression was never assessed; therefore, to the best of our knowledge, this is the first evidence about the expression of these subunits in peripheral glial cells. The expression of GABA subunits has recently been analysed in mature oligodendrocytes [37]. Indeed, it was reported that the subunits more importantly expressed are α3, β2, β3, γ1 and γ3, with the δ subunit only being expressed at very low, barely detectable, levels. This suggests that the myelinating cells of the peripheral and the central nervous system present a different pool of GABA-A subunits. We showed that SCs express extra-synaptic subunits, in particular the δ subunit, important for neuroactive steroid affinity [38]. Conversely, oligodendrocytes express almost exclusively synaptic subunits. Therefore, taken together, these data suggest that SCs and oligodendrocytes express GABA-A receptors with different subunit composition, thus displaying a different pharmacological profile.

Recent studies demonstrated a cross-talk between the GABA receptor system, indicating that GABA-A and GABA-B receptors are involved in a complex cross-regulation in the nervous system, for instance in the hypothalamus [39]. This cross-interaction has been previously hypothesised also in the PNS, where it was proposed that GABA-A and GABA-B receptors might exert opposite effects on SCs pathophysiology [40].

Our findings also suggest that the synaptic receptors may be more importantly expressed in DRGs, in line with previously reported data in which the most common receptor composition was α2β3γ2 [41], while extra-synaptic receptors seemed to be predominant in SCs.

Although some studies reported the GABA-A-mediated modulation of GABA-B receptor expression [36], little is known about GABA-A modulation through GABA-B activation/de-activation. The analysis of GABA-A receptor modulation in the P0-GABA-B1$^{fl/fl}$ model may help to explain some of the changes observed in the PNS in vivo [1].

Observing GABA-A subunit expression in dissociated DRG neurons, it is evident how these animals show a general GABA-A downregulation. This evidence suggests a reduced GABAergic inhibitory tone, which may contribute to the hyperalgesic and allodynic state observed [1]. Indeed, increased DRG neurons excitability was reported to play a role in the initiation and maintenance of central sensitisation, which is an important contributor to the development of neuropathic pain [42]. It was also reported that the neuropathy following peripheral nerve injury involves GABA-A reduced expression in sensory neurons [43]. Moreover, the silencing of α2 subunit in rat DRG proved able to worsen mechanical and thermal hypersensitivity in crush-injured rats, as well as endogenous GABA up-regulation and alleviated neuropathic pain symptoms [44].

A deepened analysis of the subunits involved in this modulation evidenced that GABA-B conditional knockout in the SCs of P0-GABA-B1$^{fl/fl}$ has an effect on both synaptic (α3) and extra-synaptic (α4 and δ) subunits in DRG neurons, while only the synaptic subunit α3 was affected in SCs. Interestingly, the strong specific reduction of α4 and δ

subunits (typically forming the most common extra-synaptic receptor [24]) in DRG neurons may suggest a specific down-regulation of δ containing extra-synaptic receptors. The δ-containing GABA-A receptors have high affinity for GABA and neuroactive steroids, and are the most important targets of the neuroactive steroid allopregnanolone [23, 45]. Alteration of their expression levels have been correlated with nociception in spinal neurons [46], but their role in DRG has not been elucidated yet. Altogether, these data shed some light on GABA-A receptor composition in the PNS, suggesting for the first time the presence of extra-synaptic subunits in SCs, thereby giving a possible explanation for the altered nociception observed in P0-GABA-B1$^{fl/fl}$ mice. The identification of alternative mechanisms involving GABA and GABA-A receptors in the modulation of peripheral pain is the matter of ongoing studies in our laboratory.

In conclusion, our observations strongly supported previous hypothesis in vivo demonstrating that GABA-B1-related changes in PNS are either SC autonomous or non-autonomous, whereas axonal and neuronal changes may occur. These effects compromise the myelination of small-diameter fibres supporting a GABA-B role in the maturation of SCs towards the non-myelinating phenotype, emphasising a role for GABA-B in the pathogenesis of neuropathic pain [47]. Interestingly, the identification of the transcriptomic profile of GABA-B1 null SCs opens new perspective in the identification of the importance of this receptor in SC biological processes.

Acknowledgements The authors are grateful to Astrid Williams for proofreading and Marinella Ballabio for technical support.

Author Contributions A.F. performed animal crossing, genotyping and culture set-up; he also performed IIC; S.M. performed cell biology experiments (proliferation, migration, etc.); V.B. and D.C. set up the co-culture experiments; L.F.C. performed GABA-A qRT-PCRs; P.M. participated in the transcriptomic analysis; M.J.A-B. and R.R. performed transcriptomic in silico analysis and statistics; V.M. supervised all experiments and wrote the manuscript with A.F.

Funding This work was supported by a grant from MIUR 'Progetto Eccellenza' and institutional grant from Università degli Studi di Milano (to V.M.); by grants from the Ministry of Economy and Competitiveness, Spain, MINECO BFU 2016-7798-P; and from Diputación Foral de Gipuzkoa, Spain DFG15/15 and DFG141/16 (to M.J.A.-B.).

Compliance with Ethical Standards

All animal experiments were conducted in accordance with the European Communities Council Directive (2010/63) and were approved by the local ethical committee of the University of Milan.

Conflict of Interest The authors have no other relevant affiliations or financial involvements with any organisation or entity with a financial interest in or financial conflict with the subjects discussed in the manuscript.

References

1. Faroni A, Castelnovo LF, Procacci P, Caffino L, Fumagalli F, Melfi S, Gambarotta G, Bettler B et al (2014) Deletion of GABA-B receptor in Schwann cells regulates Remak bundles and small nociceptive C-fibers. GLIA 62(4):548–565
2. Magnaghi V, Parducz A, Frasca A, Ballabio M, Procacci P, Racagni G, Bonanno G, Fumagalli F (2010) GABA synthesis in Schwann cells is induced by the neuroactive steroid allopregnanolone. J Neurochem 112(4):980–990
3. Perego C, Di Cairano ES, Ballabio M, Magnaghi V (2012) Neurosteroid allopregnanolone regulates EAAC1-mediated glutamate uptake and triggers actin changes in Schwann cells. J Cell Physiol 227(4):1740–1751
4. Faroni A, Terenghi G, Magnaghi V (2012) Expression of functional gamma-aminobutyric acid type a receptors in Schwann-like adult stem cells. J Mol Neurosci 47(3):619–630
5. Faroni A, Calabrese F, Riva MA, Terenghi G, Magnaghi V (2012) Baclofen modulates the expression and release of neurotrophins in Schwann-like adipose stem cells. J Mol Neurosci
6. Procacci P, Ballabio M, Castelnovo LF, Mantovani C, Magnaghi V (2012) GABA-B receptors in the PNS have a role in Schwann cells differentiation? Front Cell Neurosci 6:68
7. Magnaghi V, Procacci P, Tata AM (2009) Chapter 15: Novel pharmacological approaches to Schwann cells as neuroprotective agents for peripheral nerve regeneration. Int Rev Neurobiol 87:295–315
8. Magnaghi V, Ballabio M, Camozzi F, Colleoni M, Consoli A, Gassmann M, Lauria G, Motta M et al (2008) Altered peripheral myelination in mice lacking GABAB receptors. Mol Cell Neurosci 37(3):599–609
9. Corell M, Wicher G, Radomska KJ, Daglikoca ED, Godskesen RE, Fredriksson R, Benedikz E, Magnaghi V et al (2015) GABA and its B-receptor are present at the node of Ranvier in a small population of sensory fibers, implicating a role in myelination. J Neurosci Res 93(2):285–295
10. Magnaghi V, Castelnovo LF, Faroni A, Cavalli E, Caffino L, Colciago A, Procacci P, Pajardi G (2014) Nerve regenerative effects of GABA-B ligands in a model of neuropathic pain. Biomed Res Int 2014:368678
11. Haller C, Casanova E, Muller M, Vacher CM, Vigot R, Doll T, Barbieri S, Gassmann M et al (2004) Floxed allele for conditional inactivation of the GABAB(1) gene. Genesis 40(3):125–130
12. Feltri ML, D'Antonio M, Previtali S, Fasolini M, Messing A, Wrabetz L (1999) P0-Cre transgenic mice for inactivation of adhesion molecules in Schwann cells. Ann N Y Acad Sci 883:116–123
13. de Luca AC, Faroni A, Reid AJ (2015) Dorsal root ganglia neurons and differentiated adipose-derived stem cells: an in vitro co-culture model to study peripheral nerve regeneration. J Vis Exp (96).
14. Melfi S, Montt Guevara MM, Bonalume V, Ruscica M, Colciago A, Simoncini T, Magnaghi V (2017) Src and phospho-FAK kinases are activated by allopregnanolone promoting Schwann cell motility, morphology and myelination. J Neurochem 141(2):165–178
15. Pfaffl MW (2001) A new mathematical model for relative quantification in real-time RT-PCR. Nucleic Acids Res 29(9):e45–e445
16. Magnaghi V, Ballabio M, Roglio I, Melcangi RC (2007) Progesterone derivatives increase expression of Krox-20 and Sox-10 in rat Schwann cells. J Mol Neurosci 31(2):149–157
17. Irizarry RA, Bolstad BM, Collin F, Cope LM, Hobbs B, Speed TP (2003) Summaries of Affymetrix GeneChip probe level data. Nucleic Acids Res 31(4):e15–e115
18. Subramanian A, Tamayo P, Mootha VK, Mukherjee S, Ebert BL, Gillette MA, Paulovich A, Pomeroy SL et al (2005) Gene set enrichment analysis: a knowledge-based approach for interpreting genome-wide expression profiles. Proc Natl Acad Sci U S A 102(43):15545–15550

19. Lawson SN (1992) Morphological and biochemical cell types of sensory neurons. Sensory neurons: diversity, development and plasticity. Oxford University Press Inc., New York.
20. Yamada H, Komiyama A, Suzuki K (1995) Schwann cell responses to forskolin and cyclic AMP analogues: comparative study of mouse and rat Schwann cells. Brain Res 681(1–2):97–104
21. Gokey NG, Srinivasan R, Lopez-Anido C, Krueger C, Svaren J (2012) Developmental regulation of microRNA expression in Schwann cells. Mol Cell Biol 32(2):558–568
22. Zhao X, He X, Han X, Yu Y, Ye F, Chen Y, Hoang T, Xu X et al (2010) MicroRNA-mediated control of oligodendrocyte differentiation. Neuron 65(5):612–626
23. Belelli D, Harrison NL, Maguire J, Macdonald RL, Walker MC, Cope DW (2009) Extrasynaptic GABAA receptors: form, pharmacology, and function. J Neurosci 29(41):12757–12763
24. Fritschy JM, Panzanelli P (2014) GABAA receptors and plasticity of inhibitory neurotransmission in the central nervous system. Eur J Neurosci 39(11):1845–1865
25. Melcangi RC, Magnaghi V, Cavarretta I, Zucchi I, Bovolin P, D'Urso D, Martini L (1999) Progesterone derivatives are able to influence peripheral myelin protein 22 and P0 gene expression: possible mechanisms of action. J Neurosci Res 56(4):349–357
26. Iacovelli J, Lopera J, Bott M, Baldwin E, Khaled A, Uddin N, Fernandez-Valle C (2007) Serum and forskolin cooperate to promote G1 progression in Schwann cells by differentially regulating cyclin D1, cyclin E1, and p27Kip expression. Glia 55(16):1638–1647
27. Rahmatullah M, Schroering A, Rothblum K, Stahl RC, Urban B, Carey DJ (1998) Synergistic regulation of Schwann cell proliferation by heregulin and forskolin. Mol Cell Biol 18(11):6245–6252
28. Han D, Choi MR, Jung KH, Kim N, Kim SK, Chai JC, Lee YS, Chai YG (2015) Global transcriptome profiling of genes that are differentially regulated during differentiation of mouse embryonic neural stem cells into astrocytes. J Mol Neurosci 55(1):109–125
29. Braunewell KH, Pesheva P, McCarthy JB, Furcht LT, Schmitz B, Schachner M (1995) Functional involvement of sciatic nerve-derived versican- and decorin-like molecules and other chondroitin sulphate proteoglycans in ECM-mediated cell adhesion and neurite outgrowth. Eur J Neurosci 7(4):805–814
30. Werle MJ (2008) Cell-to-cell signaling at the neuromuscular junction: the dynamic role of the extracellular matrix. Ann N Y Acad Sci 1132:13–18
31. Terauchi A, Johnson-Venkatesh EM, Toth AB, Javed D, Sutton MA, Umemori H (2010) Distinct FGFs promote differentiation of excitatory and inhibitory synapses. Nature 465(7299):783–787
32. Bremer J, O'Connor T, Tiberi C, Rehrauer H, Weis J, Aguzzi A (2010) Ablation of dicer from murine Schwann cells increases their proliferation while blocking myelination. PLoS One 5(8):e12450
33. Pereira JA, Baumann R, Norrmen C, Somandin C, Miehe M, Jacob C, Luhmann T, Hall-Bozic H et al (2010) Dicer in Schwann cells is required for myelination and axonal integrity. J Neurosci 30(19):6763–6775
34. Yun B, Anderegg A, Menichella D, Wrabetz L, Feltri ML, Awatramani R (2010) MicroRNA-deficient Schwann cells display congenital hypomyelination. J Neurosci 30(22):7722–7728
35. Svaren J (2014) MicroRNA and transcriptional crosstalk in myelinating glia. Neurochem Int 77:50–57
36. Magnaghi V, Ballabio M, Consoli A, Lambert JJ, Roglio I, Melcangi RC (2006) GABA receptor-mediated effects in the peripheral nervous system: a cross-interaction with neuroactive steroids. J Mol Neurosci 28(1):89–102
37. Arellano RO, Sanchez-Gomez MV, Alberdi E, Canedo-Antelo M, Chara JC, Palomino A, Perez-Samartin A, Matute C (2016) Axon-to-glia interaction regulates GABAA receptor expression in oligodendrocytes. Mol Pharmacol 89(1):63–74
38. Belelli D, Lambert JJ (2005) Neurosteroids: endogenous regulators of the GABA(a) receptor. Nat Rev Neurosci 6(7):565–575
39. Wright R, Newey SE, Ilie A, Wefelmeyer W, Raimondo JV, Ginham R, McLlhinney RAJ, Akerman CJ (2017) Neuronal chloride regulation via KCC2 is modulated through a GABAB receptor protein complex. J Neurosci 37(22):5447–5462
40. Faroni A, Magnaghi V (2011) The neurosteroid allopregnanolone modulates specific functions in central and peripheral glial cells. Front Endocrinol (Lausanne) 2:103
41. Ma W, Saunders PA, Somogyi R, Poulter MO, Barker JL (1993) Ontogeny of GABAA receptor subunit mRNAs in rat spinal cord and dorsal root ganglia. J Comp Neurol 338(3):337–359
42. Julius D, Basbaum AI (2001) Molecular mechanisms of nociception. Nature 413(6852):203–210
43. Obata K, Yamanaka H, Fukuoka T, Yi D, Tokunaga A, Hashimoto N, Yoshikawa H, Noguchi K (2003) Contribution of injured and uninjured dorsal root ganglion neurons to pain behavior and the changes in gene expression following chronic constriction injury of the sciatic nerve in rats. Pain 101(1–2):65–77
44. Obradovic AL, Scarpa J, Osuru HP, Weaver JL, Park JY, Pathirathna S, Peterkin A, Lim Y et al (2015) Silencing the alpha2 subunit of gamma-aminobutyric acid type a receptors in rat dorsal root ganglia reveals its major role in antinociception posttraumatic nerve injury. Anesthesiology 123(3):654–667
45. Carver CM, Reddy DS (2013) Neurosteroid interactions with synaptic and extrasynaptic GABA(a) receptors: regulation of subunit plasticity, phasic and tonic inhibition, and neuronal network excitability. Psychopharmacology 230(2):151–188
46. Bonin RP, Labrakakis C, Eng DG, Whissell PD, De Koninck Y, Orser BA (2011) Pharmacological enhancement of delta-subunit-containing GABA(a) receptors that generate a tonic inhibitory conductance in spinal neurons attenuates acute nociception in mice. Pain 152(6):1317–1326
47. Dutsch M, Marthol H, Stemper B, Brys M, Haendl T, Hilz MJ (2002) Small fiber dysfunction predominates in Fabry neuropathy. J Clin Neurophysiol 19(6):575–586